Research papers

Reactive transport modelling to infer changes in soil hydraulic properties induced by non-conventional water irrigation

Javier Valdes-Abellan[a, *]

javier.valdes@ua.es

Joaquín Jiménez-Martínez[b, c]

Lucila Candela[d]

Diederik Jacques[e]

Claus Kohfahl[f]

Karim Tamoh[d]

[a]Department of Civil Engineering, University of Alicante, Alicante, Spain

[b]Department Water Resources and Drinking Water, Swiss Federal Institute of Aquatic Science and Technology (EAWAG), Dubendorf, Switzerland

[c]Department of Civil, Environmental and Geomatic Engineering, Swiss Federal Institute of Technology (ETH), Zurich, Switzerland

[d]Department of Civil and Environmental Engineering, Technical University of Catalonia, Barcelona, Spain

[e]Institute for Environment, Health and Safety, Belgian Nuclear Research Center (SCK-CEN), Mol, Belgium

[f]Geological Survey of Spain, Sevilla-Office, Sevilla, Spain

*Corresponding author.

This manuscript was handled by Corrado Corradini, Editor-in-Chief, with the assistance of Christophe Darnault, Associate Editor

Abstract

The use of non-conventional water (e.g., treated wastewater, desalinated water) for different purposes is increasing in many water scarce regions of the world. Its use for irrigation may have potential drawbacks, because of mineral dissolution/precipitation processes, such as changes in soil physical and hydraulic properties (e.g., porosity, permeability), modifying infiltration and aquifer recharge processes or blocking root growth. Prediction of soil and groundwater impacts is essential for achieving sustainable agricultural practices. A numerical model to solve unsaturated water flow and non-isothermal multicomponent reactive transport has been modified implementing the spatio-temporal evolution of soil physical and hydraulic properties. A long-term process simulation (30 years) of agricultural irrigation with desalinated water, based on a calibrated/validated 1D numerical model in a semi-arid region, is presented. Different scenarios conditioning reactive transport (i.e., rainwater irrigation, lack of gypsum in the soil profile, and lower partial pressure of CO_2 (pCO_2)) have also been considered. Results show that although boundary conditions and mineral soil composition highly influence the reactive processes, dissolution/precipitation of carbonate species is triggered mainly by pCO_2, closely related to plant roots. Calcite dissolution occurs in the root zone, precipitation takes place under it and at the soil surface, which will lead a root growth blockage and a direct soil evaporation decrease, respectively. For the studied soil, a gypsum dissolution up to 40 cm depth is expected at long-term, with a general increase of porosity and hydraulic conductivity.

Keywords: Soil; Non-conventional water; Reactive transport; Physical properties; Hydraulic properties

1 Introduction

Irrigation with non-conventional or low-quality water (treated wastewater, TWW; desalinated water, DW) in arid and semi-arid regions, where water scarcity forces farmers to consider alternative sources, is becoming an increasingly widespread practise in

agricultural management to achieve food security (MedWSD Working Group, 2007; Qadir et al., 2007; Tal, 2006). TWW is one of the first non-conventional water resources to be used for irrigation since wastewater treatment is compulsory in the vast majority of developed countries. More recently, use of desalinated water has increased in some developed countries, forced by the high demand of fresh water. Desalinated water cost is affordable for some uses (e.g., drinking water), but still remains costly for agricultural uses (Martínez Beltrán and Koo-Oshima, 2004). A normal practise to re-mineralise DW and to increase the final water volume is to mix DW with the original saline water (Valdes-Abellan et al., 2013) to thus, lower the cost.

Impacts on soil properties from using non-conventional water for irrigation have been widely studied in recent years. Some studies have focused on vadose zone impacts from TWW-based irrigation (Assouline and Narkis, 2013; Lahav et al., 2010; Xu et al., 2010). Reduction in hydraulic conductivity close to the soil surface, along with low salt leaching and built-up salinity in the soil profile have been observed. Clogging processes, similar to those observed from artificial recharge, have also been reported (Bouwer, 2002; Sani et al., 2013). Soil impact studies from highly mineralised water have been addressed mainly by soil columns under laboratory conditions (Lado and Ben-Hur, 2010), while only few detailed studies at field scale, including soil improvement research (e.g., Reading et al., 2012a), have been carried out (e.g., Costa, 1999; Minhas et al., 1994). Most research has established a relationship between water quality in terms of sodium adsorption rates (*SAR*) and electrical conductivity (*EC*) and hydraulic conductivity changes. As far as we know, long-term impact studies on soil from irrigation with intermediate water qualities are lacking. Finally, irrigation with wastewater or desalinated water often introduces inorganic, organic or biological contaminants, which lead to soil degradation and so their consequences are of great environmental concern (Valdes-Abellan et al., 2013).

Modelling variable-saturated flow and reactive transport is an efficient tool to assess the long-term impacts on soil caused by wastewater and saline water application. Modelling approaches have focused on salinity evolution in soil (Kanzari et al., 2012), impact on crop yields (Phogat et al., 2010; Ramos et al., 2011), and a few on soil hydraulic properties (Assouline and Narkis, 2011; Reading et al., 2012b). Most previous research works have focused on possible impacts with a limited type of processes, and did not consider precipitation/dissolution processes, heat flux or changes in soil physical and hydraulic properties. For accurate and reliable model prediction, it is necessary to consider all the processes involved in coupling unsaturated flow, non-isothermal multicomponent reactive transport, and transient soil physical and hydraulic properties (Šimůnek et al., 2006; Wissmeier and Barry, 2009; Steefel et al., 2015).

The main objective of this research is to assess possible long-term changes in soil physical and hydraulic properties from the use of non-conventional water for irrigation. The HP1 code (Jacques et al., 2006, 2008) to simulate unsaturated water flow and non-isothermal multicomponent reactive transport has been adapted to include the spatio-temporal evolution of soil physical and hydraulic properties as a result of the minerals dissolution/precipitation. It includes porosity, soil hydraulic conductivity and alpha parameter (inverse of air entry value) from the van Genuchten model. A long-term prediction (30 years) of flow and reactive transport processes in the vadose zone of a grass plot irrigated with desalinated water (slight saline) is presented herein. For that purpose, 3 years of field data, along with a calibrated/validated flow, solute and heat transport model have been used for the long-term predictions. Alternative scenarios as rainwater irrigation, lack of gypsum in the soil profile, and lower partial pressure of CO_2 (pCO_2) than measured in the soil are also considered. This work also aims at assessing possible impacts on vegetation, i.e., root growth blockage, and to shed light on the agricultural management options.

2 Numerical modelling

Unsaturated water flow, mass and heat transport are simulated with the HYDRUS-1D code (Šimůnek et al., 2009). The HP1 code (Jacques et al., 2008) for solving non-isothermal multicomponent reactive transport is applied. HP1 couples HYDRUS-1D with the hydrogeochemical code PHREEQC (Parkhurst and Appelo, 2013). This research uses a non-released beta version of HP1, which includes in the modelling process the spatio-temporal variability of soil physical and hydraulic properties (Fig. 1).

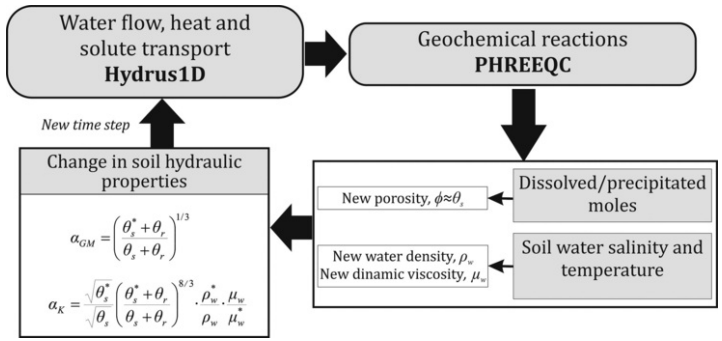

Fig. 1 Non-isothermal reactive transport modelling flowchart.

2.1 Water flow

Unsaturated water flow is modelled according to Richards' equation (Richards, 1931):

$$\frac{\partial \theta}{\partial t} = \frac{\partial}{\partial z}\left(K(\theta)\left(\frac{\partial h}{\partial z} + 1\right)\right) - S \quad (1)$$

where θ is volumetric water content ($L^3\ L^{-3}$); t time (T); z the vertical space dimension (L); $K(\theta)$ unsaturated hydraulic conductivity function of soil ($L\ T^{-1}$); h soil pressure head (L); and S a sink term that represents water uptake by plants ($L^3\ L^{-3}\ T^{-1}$). The soil hydraulic properties are defined by van Genuchten-Mualem constitutive relationships (Mualem, 1976; van Genuchten, 1980):

$$\theta(h) = \begin{cases} \theta_r + \frac{\theta_{s,upd} - \theta_r}{[1+|\alpha_{upd}h|^n]^{1-1/n}} & h<0 \\ \theta_{s,upd} & h \geqslant 0 \end{cases} \quad (2)$$

$$K(h) = KupdSe^l\{1-[1-Se^{n/(n-1)}]^{1-1/n}\}^2 \quad K\left(h\right) = K_{upd}S_e{}^l\left\{1-\left[1-S_e{}^{n/(n-1)}\right]^{1-1/n}\right\}^2 \quad (3)$$

where S_e is effective saturation:

$$S_e = \frac{\theta(h) - \theta_r}{\theta_{s,upd} - \theta_r} \quad (4)$$

and $\theta_{s,upd}$ the modified saturated water content ($L^3\ L^{-3}$); θ_r the residual water content ($L^3\ L^{-3}$); K_{upd} new saturated hydraulic conductivity ($L\ T^{-1}$); and α_{upd} (L^{-1}), n (–), and l (–) the empirical coefficients that determine the shape of the hydraulic functions, being α updated in each computational time step. In order to avoid over-parametrisation, l = 0.5 is commonly assumed, based on Mualem (1976).

2.2 Heat transport

Heat transport modelling is performed after taking into account the different equilibrium constants of the mineral phases and soil temperature. The governing heat transport equation is:

$$\frac{\partial C_p(\theta)T}{\partial t} = \frac{\partial}{\partial x}\left(\lambda(\theta)\frac{\partial T}{\partial x}\right) - C_w\frac{\partial qT}{\partial x} - C_wST \quad (5)$$

where the new parameters are: T temperature of soil (K, T); C_w and C_p volumetric heat capacity of the liquid phase and the porous medium (de Vries, 1963), respectively ($J\ m^{-3}\ K^{-1}$, $M\ L^2\ T^{-2}$); $\lambda(\theta)$ apparent thermal conductivity of soil ($J\ s^{-1}\ m^{-1}\ K^{-1}$, $M\ L\ T^{-3}\ K^{-1}$); q volumetric water flux density ($L\ T^{-1}$), and the rest of parameters are previously defined. The three terms on the right represent heat transfer by conduction, heat transport by water, and energy uptake by plant roots associated with root water uptake, respectively.

The apparent thermal conductivity combines the thermal conductivity $\lambda_0(\theta)$ of the porous medium (solids plus water) with flow-induced macrodispersivity (de Marsily, 1986):

$$\lambda(\theta) = \lambda_0(\theta) + \beta_t C_w|q| \quad (6)$$

where β_t is thermal dispersivity (L). The volumetric heat capacity of liquid phase incorporates the thermal conductivity notation after the rearrangement of the thermal dispersivity length units (Chung and Horton, 1987):

$$\lambda_0(\theta) = \omega_1 + \omega_2\theta + \omega_3\theta^{0.5} \quad (7)$$

where ω_1, ω_2, and ω_3 are empirical parameters ($M\ L\ T^{-3}\ K^{-1}$).

2.3 Multicomponent reactive transport

The advection-dispersion equation, with the additional reactive term to take into account geochemical processes, is used to solve transport:

$$\frac{d(\theta C_i)}{dt} = \frac{\partial}{\partial z}(\theta D_i\frac{\partial C_i}{\partial z}) - \frac{\partial(q_z C_i)}{\partial z} - SC_{r,i} + R_i; \quad \frac{d(\rho s_i)}{dt} = -R_i \quad (8)$$

where ρ is bulk density of the porous media ($M\ L^{-3}$); s solute i concentration in the solid phase ($M\ M^{-1}$); C_i aqueous concentration of element i ($M\ L^{-3}$); D dispersion coefficient of element i in the liquid phase ($L^2\ T^{-1}$); $C_{r,i}$ concentration of element i of the sink term ($M\ L^{-3}$); R_i is a source/sink term of element i due to heterogeneous geochemical reactions ($M\ L^{-3}\ T^{-1}$).

The dispersion coefficient in the liquid phase, D, represents the combined effects of dispersion and molecular diffusion:

$$D = \eta\frac{|q|}{\theta} + D_m\tau \quad (9)$$

where η is dispersivity (L); D_m temperature-dependent ions diffusion coefficient ($L^{-2}\ T^{-1}$); τ tortuosity (dimensionless), calculated as $\tau = \theta^{7/3}/\theta_s^2$ (Millington and Quirk, 1961).

Reactive solute transport, as defined, involved a number of interrelated processes and dependent parameters depending on the state of the system. The effect of temperature on the diffusion coefficients and equilibrium constants, i.e., the non-isothermal

character, is also considered (Appelo and Postma, 2005; Parkhurst and Appelo, 2013).

2.4 Soil properties changes

HP1 allows changes of flow and transport parameters induced by changes in the geochemical state variables (e.g., Jacques et al., 2011; Xie et al., 2015; Francisca and Glatstein, 2010). In this research, and as main new implementation in this well-known numerical tool, variation of porosity in soil media is estimated after each geochemical computational step by considering the balance between the amount of precipitated and dissolved minerals. The hydraulic conductivity and van Genuchten alfa parameter scaling factors, α_{GM} (–) and α_K (–), respectively, at each location in the soil profile are computed according to Wissmeier and Barry (2009, 2010). Note that porosity is assumed to be the saturated volumetric water content, $\phi \approx \theta_s$. Therefore, the scaling factors are as follow:

$$\alpha_{GM} = \left(\frac{\theta_s^* + \theta_r}{\theta_s + \theta_r}\right)^{1/3} \quad (10)$$

$$\alpha_{K1} = \frac{\sqrt{\theta_s^*}}{\sqrt{\theta_s}}\left(\frac{\theta_s^* + \theta_r}{\theta_s + \theta_r}\right)^{8/3} \quad (11)$$

where $*$ denotes the new values after mineral reactions.

On the other hand, water salinity and temperature are used to estimate the potential changes in water density (Eq. (12)) and dynamic viscosity (Eq. (13)), and their influence on the hydraulic conductivity as consequence. They are respectively as (e.g., Sharqawy et al., 2010):

$$\rho_W = (a_1 + a_2 \cdot T + a_3 \cdot T^2 + a_4 \cdot T^3 + a_5 \cdot T^4) + (b_1 + b_2 \cdot T \cdot s_s + b_3 \cdot T^2 \cdot s_s + b_4 \cdot T^3 \cdot s_s + b_5 \cdot T^4 \cdot s_s^2) \quad (12)$$

where $a_1 = 9.999 \cdot 10^2$; $a_2 = 2.034 \cdot 10^{-2}$; $a_3 = -6.162 \cdot 10^{-3}$; $a_4 = 2.261 \cdot 10^{-5}$; $a_5 = -4.657 \cdot 10^{-8}$; $b_1 = 8.020 \cdot 10^2$; $b_2 = -2.001$; $b_3 = 1.677 \cdot 10^{-2}$; $b_4 = -3.060 \cdot 10^{-5}$; $b_5 = -1.613 \cdot 10^{-5}$; T is temperature (Celsius); ~~and~~ s_s is salinity (kg · kg^{-1}); and

$$\mu_w = \mu \cdot (1 + A \cdot s_s + B \cdot s_s^2) \quad (13)$$

where $\mu = 4.2844 \cdot 10^{-5} + [0.157 \cdot (T + 64.993)^2 - 91.296]^{-1}$; $A = 1.541 + 1.998 \cdot 10^{-2} \cdot T - 9.52 \cdot 10^{-5} \cdot T$; and $B = 7.974 - 7.561 \cdot 10^{-2} \cdot T + 4.724 \cdot 10^{-4} \cdot T^2$. The scaling factor for hydraulic conductivity is obtained through the relation between hydraulic conductivity and intrinsic permeability of the porous media

$$\alpha_{K2} = \frac{\rho_w^*}{\rho_w} \cdot \frac{\mu_w}{\mu_w^*} \quad (14)$$

where $*$ denotes the new values after mineral reactions.

Therefore, the updated van Genuchten alpha parameter and saturated hydraulic conductivity (in Eqs. (2) and (3)) are as:

$$\alpha_{upd} = \alpha_0 \cdot \alpha_{GM} \quad (15)$$

$$K_{upd} = K_0 \cdot \alpha_{K1} \cdot \alpha_{K2} \quad (16)$$

where subscript 0 denotes the initial values, and the subscript *upd* denotes the new values at each node of the modelled soil profile.

With the new calculated values of van Genuchten alpha parameter and saturated hydraulic conductivity, Hydrus 1D solves in a coupled way water flow, solute and heat transport (Šimůnek et al., 2009).Subsequently, the PHREEQC code is called and all potential hydrogeochemical reactions taking place in the soil media, including fluid-fluid and fluid-solid reactions, are computed. In the next step, once the dissolved and precipitated species are known, porosity is recalculated at each depth. Similarly, soil water density and viscosity data are updated according to geochemical speciation and heat transport results. The updated values of porosity distribution along depth (assumed equal to the saturated water content) and soil water density and viscosity are used to compute the changes in the soil hydraulic properties, including van Genuchten alpha parameter and saturated hydraulic conductivity, prior to the next time step (Fig. 1).

3 Field site and experiment

3.1 Experimental site

The field experiment was conducted on an experimental plot set up in Alicante (SE Spain). The area is characterised by a semi-arid Mediterranean climate with dry hot summers and mild winters: 18 °C mean annual temperature and a precipitation rate of 330 mm yr^{-1}. Rainfall takes place mainly in spring and autumn, when intense rainfall events occur. The mean annual reference evapotranspiration, ET_0, according to Penman-Monteith (Allen et al., 1998) accounted for ~1278 mm.

The experimental plot (9 × 5 m^2) is cultivated with a mixture of turf grass species (St. Agustine grass, *Stenotaphrumsecundatum*, and ray grass, *Loliumperenne*) to mimic landscape management. It is irrigated with desalinated water by micro-sprinklers (from summer

2011 to present time), with a mean annual value of 1550 mm (Valdes-Abellan et al., 2013). The monitoring of the volumetric soil water content and soil temperature has been done by sensors at depths of 20, 40, 60, 90 and 120 cm. Temperature of the top soil surface has been also monitored by a sensor located at 1 cm depth, in order to establish the upper boundary condition. The soil pressure head has been controlled only at depths of 20 and 60 cm. A detailed description of the experimental plot and installed devices can be found in Valdes-Abellan et al. (2015).

3.2 Characterization of the soil properties

Physical and hydraulic soil properties have been determined from disturbed and undisturbed soil cores taken at different depths. The laboratory determinations included: soil bulk density according to (Grossman and Reinsch, 2002), porosity (Flint and Flint, 2002), particle size distribution (Gee and Or, 2002), saturated and residual volumetric water content, saturated hydraulic conductivity (Reynolds and Elrick, 2002) and soil water retention curves, SWRC (Dane and Hopmans, 2002).

The chemical properties of soil media have been determined from disturbed samples. The soil chemical composition and soil mineralogy have been obtained by X-ray fluorescence, XRFS (Abderrahim et al., 2011; Brindley and Brown, 1980) and X-ray diffractometry (Jones, 1991), respectively. Cation exchange capacity, *CEC*, has been determined according to Sumner and Miller (1996), while organic carbon, *OM*, based on Nelson and Sommers (1996).

3.3 Irrigation water quality

Irrigation is carried out with a mix of desalinated water (DW) from an inland brackish aquifer (Prats and Chillón Arias, 2001; Prats et al., 1997) and the groundwater that is pumped directly from the aquifer (see Supplementary Material). The desalination process includes a post-treatment stage with $Ca(OH)_2$ addition to meet Spanish Ca^{2+} and HCO_3^- concentration requirements (Royal Decree 1138/1990). Mixing brackish groundwater and DW is quite variable, with the fraction of raw groundwater ranging between 5% and 22% in winter and summer, respectively (Valdes-Abellan et al., 2013).

Irrigation water sampling has been carried out monthly. Chemical determinations, including major ions and physicochemical parameters, have been done following standards procedures, while *in situ* determinations have been carried out with a multiparameter recording device, which includes pH, temperature, redox potential (*Eh*) and electrical conductivity.

The saturation index, *SI,* for the relevant minerals and ionic species has been calculated after considering atmospheric conditions (i.e., pCO_2 equalled $10^{-3.5}$ atm) with the PHREEQCi-3.1.7 code (Parkhurst and Appelo, 2013), based on minteq.v4.dat as the thermodynamic database (Ball and Nordstrom, 1991).

4 Model application

4.1 Main scenario

A 140 cm deep soil profile and three soil layers have been defined according to the soil characterisation results of the experimental plot (Table 1 and Fig. 2). The horizontal uniformity (i.e., homogeneous and isotropic) observed across the experimental plot allows to consider a one-dimensional model. A 30 years numerical simulation with HP1 has been performed to predict the geochemically-induced (mineral kinetics) long-term changes in soil physical and hydraulic properties.

Table 1 Summary of the soil physical, hydraulic and transport properties.

Layer	1	2	3
Depth (m)	0–0.05	0.05–0.39	0.39–1.40
Sand/Silt/Clay (%)	36.2/29.6/34.2	59.1/34.8/6.0	45.4/47.1/7.5
Texture	Clay loam	Sandy loam	Loam
Bulk density, ρ (g cm^{-3})	1.38	1.5	1.42
Porosity (%)	47	41	44
Particle density (g cm^{-3})	2.65	2.53	2.54
θ_s (cm^3 cm^{-3})*	0.48	0.39	0.41
θ_r (cm^3 cm^{-3})*	0.04	0.15	0.15
α (cm^{-1})*	$5.11 \cdot 10^{-3}$	$2.47 \cdot 10^{-2}$	$1.66 \cdot 10^{-2}$

n (–)*	1.90	1.48	1.42
K_s (cm day^{-1})*	5.9	50	60.9
Dispersivity, η (cm)**	2.44	14.99	1.83

*From Valdes-Abellan et al. (2015).

**From Valdes-Abellan et al. (2014).

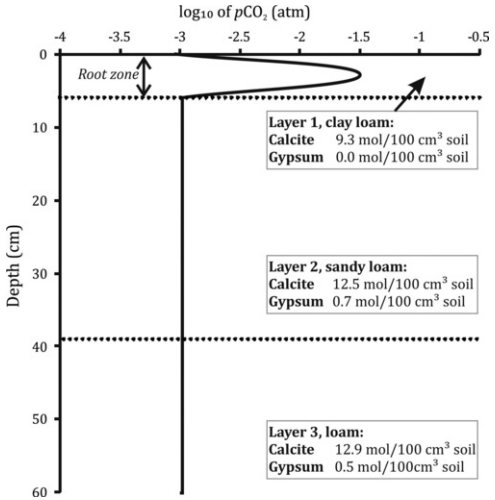

Fig. 2 Initial pCO_2 profile and volumetric concentration for the two more abundant minerals (calcite and gypsum) in the three defined soil layers.

A calibrated/validated water flow model from soil water content and pressure head observations along three years is used as initial soil parameterization (Table 1) (Valdes-Abellan et al., 2015). At the top, atmospheric boundary condition (potential evapotranspiration, water input and root water uptake) are considered, while free drainage is assumed as the lower boundary condition since water table is far below the domain. Root depth is considered constant, 6 cm, while for potential evapotranspiration ET_p, according to Penman-Monteith, 10 cm height is considered for the cultivated grass species on the plot. Root water stress was modelled by the modified Feddes model (Wesseling and Brandyk, 1985; Feddes et al., 1978). The original Feddes model considers a maximum water uptake between h_2 and h_3, zero water uptake when soil pressure head is below and above two boundary levels, h_4 and h_1, respectively, and linear transitions between these domains. A double value of h_3 depending on the potential water uptake is considered in the modified Feddes model (Wesseling and Brandyk, 1985) (Fig. 3). The values adopted for the current crop (grass) are: h_1 = −10 cm; h_2 = −25 cm; $h_{3.1}$ = −240 cm; $h_{3.2}$ = −360 cm; and h_4 = −8000 cm. And the threshold values of evaporation to trigger $h_{3.1}$ or $h_{3.2}$ values are 1 mm day^{-1} and 5 mm day^{-1} (i.e., if ET_p > 5 mm day^{-1}, then $h_{3.2}$ is used, while if ET_p < 1 mm day^{-1}, then $h_{3.1}$ is used).

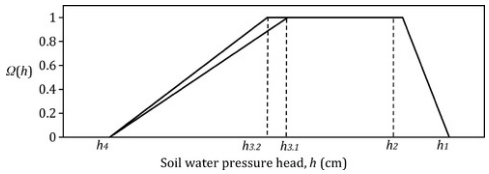

Fig. 3 Root water uptake Feddes-Wesseling model scheme. $\Omega(h)$ is the dimensionless water stress response function ($0 \le \Omega(h) \le 1$) that prescribes the reduction in uptake that occurs due to drought stress.

Soil thermal properties (Table 2) have been obtained from a calibrated heat transport model, and by inverse method, for the period 1 September 2011–30 ~~Abril~~April 2013. The measured and simulated temperature results, at different depths for the calibration period, are included in the Supplementary Material.

Table 2 Soil thermal properties of the three defined soil layers.

Layer	1	2	3

Longitudinal thermal dispersivity, β_t (cm)	1	1	1
b_1 (W m^{-1} K^{-1})	−0.197	0.206	0.281
b_2 (W m^{-1} K^{-1})	−0.962	0.393	0.451
b_3 (W m^{-1} K^{-1})	2.521	1.534	1.534
Volumetric heat capacity of the solid phase, C_s (J m^{-3} K^{-1})	$2.013 \cdot 10^6$	$1.648 \cdot 10^6$	$2.251 \cdot 10^6$

For the multicomponent reactive transport, dissolution and precipitation of five mineral species are considered: dolomite, calcite, aragonite, anhydrite, and gypsum (molar volumes, http://database.iem.ac.ru/mincryst/, listed in Table 3). The initial soil content (moles) of these mineral species have been derived from the mineralogical determinations. Initial equilibrium of calcite and gypsum in the soil water is considered; pCO_2 in soil is set at $10^{-1.5}$ atm in the root zone and at 10^{-3} atm below it (Appelo and Postma, 2005) after considering that biological activity diminished below this depth (Fig. 2). The rainfall presents low mineralisation, and it is considered in equilibrium with $pCO_2 = 10^{-3.5}$ atm. The dispersivity values for the different soil layers of the model have been obtained by inverse modelling of a tracer test, as described in Valdes-Abellan et al. (2014) (Table 1).

Table 3 Solid mineral phases, chemical reactions, molar volume and molar mass of the solid mineral phases considered.

Mineral	Reaction	Molar volume (cm^3 mol^{-1})	Molar mass (g mol^{-1})
Dolomite	$CaMg(CO_3)_2 = Ca^{2+} + Mg^{2+} + 2CO_3^{2-}$	64.12	184.34
Calcite	$CaCO_3 = Ca^{2+} + CO_3^{2-}$	36.93	100.06
Aragonite	$CaCO_3 = Ca^{2+} + CO_3^{2-}$	34.17	100.06
Anhydrite	$CaSO_4 = Ca^{2+} + SO_4^{2-}$	46.00	154.09
Gypsum	$CaSO_4 \cdot 2H_2O = Ca^{2+} + SO_4^{2-} + 2H_2O$	74.56	172.08

The data (precipitation, irrigation and evapotranspiration, as well as temporal and intensity distribution) collected along the Sep-11 Aug-14 period are used to generate the 30 year time future scenario data set. For this exercise, global change effects as derived from the ICCP panel are not taken into consideration, although a rise in both temperature and the intensity of extreme rainfall events in the study area are expected (Candela et al., 2009).

4.2 Considered scenarios of environmental conditions

Three different scenarios to assess soil media response to changes in the boundary and initial conditions compared to the reference scenario are studied. Proposed scenarios include representative and probable environmental conditions and agricultural practices: (*i*) *rain-fed irrigation*, with input only from precipitation, while changes in the initial conditions are not considered; (*ii*) *lack of gypsum in the soil profile*, in order to highlight the importance of gypsum in the processes, given its molar volume; (*iii*) *a lower* pCO_2 (pCO_2 of $10^{-2.5}$ atm) *in the root zone* than the reference scenario initial value; to carry out a sensitivity analysis of this parameter and, given the key role that pCO_2 (atmospherically and biologically controlled) plays in calcite precipitation and dissolution. In bare and no-tillage soils, pCO_2 can be generally lower than $10^{-1.5}$ atm (e.g., Lee, 1997; Loisy et al., 2013).

5 Results and discussion

5.1 Soil and water composition: chemical indices

Calcite is the most abundant mineral followed by quartz (Table 4) in the three defined soil layers; both minerals accounted for 85.3%, 90.5% and 90.4% composition for layer 1, 2 and 3, respectively. Compared with the other layers, layer 1 exhibits higher SiO_2 content and lower CaO content. Presence of clay minerals is practically negligible, except layer 1 where Illite content accounts for 9.7%. Gypsum is not present in layer 1, but in layers 2 and 3. The three layers have low *CEC* and *OM* contents, being slightly higher in layer 1 than in layers 2 and 3 (Table 4).

Table 4 Oxide states components of the solid phase and mineralogy for the three defined layers.

Layer	1	2	3
Calcination loss (% of weight)	40.90	38.33	35.97
Oxide states components of the solid phase, X-ray fluorescence (% of weight)			
Al_2O_3	6.43	1.73	2.98
CaO	27.15	46.00	45.67
Cl	0.10	0.09	0.05
Fe_2O_3	1.84	0.48	0.76
K_2O	1.45	0.31	0.48
MgO	2.53	2.06	1.99
MnO	0.01	0.00	0.00
Na_2O	0.40	0.20	0.18
P_2O_5	0.10	0.00	0.01
SO_3	0.17	2.94	0.95
SiO_2	18.65	7.71	10.82
TiO_2	0.26	0.02	0.06
Components of the solid phase, X-ray fluorescence (ppm)			
Ba	0.00	6.00	0.00
Br	11.50	16.75	12.00
Cu	12.00	17.25	11.00
Ni	0.00	0.00	0.00
Pb	26.50	26.00	20.33
Rb	51.50	18.75	24.33
Sr	482.00	1193.25	1193.67
Zn	37.50	19.75	15.33
Zr	100.50	39.00	87.00
Soil mineralogy reported by X-ray diffractometry (% of the solid mineral phase)			
Calcite	67.2	80.2	83.1
Quartz	18.1	10.6	7.2
Gypsum	0	9.2	4.1
Illite	9.7	0	2.9
Dolomite	5	0	0
Albite	0	0	1.2
Orthoclase	0	0	1.6

Cation exchange capacity and organic matter content			
CEC (meq·100 g^{-1})	12.4	4.7	5.8
OM (% C of dry soil weight)	0.8	0.21	0.12
OM (% oxidable *OM*)	1.38	0.36	0.22

Table 5 summarises the monthly-analysed chemical composition and physico-chemical parameters of irrigation water. The chemical balance error was always lower than 1.9%. It shows a monthly variation of the applied water, with sodium-chloride-sulphate facies at a neutral pH. The chemical indices (i.e., Hardness, TAC, *SAR*) are also computed. *SI* shows that irrigation water is subsaturated for most of the possible mineral phases within the existing pH range. Yet under atmospheric conditions, almost saturated or even oversaturated conditions (i.e., *SI* > 0) prevail for the most relevant mineral species: aragonite, calcite, dolomite, anhydrite and gypsum. The *SI* variation along a year for these minerals is shown in Fig. 4. Note the increased *SI* of Ca- and Mg-carbonate during the summer season, which indicates that mineral precipitation may occur. From the chemical indicators *SAR* and *EC*, there is a medium risk of alkalinisation for most of the water samples, while the risk of salinization is high (or even very high) in all the analysed samples (see Supplementary Material).

Table 5 Physico-chemical characteristics and major ion contents for irrigation water during the 2011–2012 period.

	January	February	March	April	May	June	July	August	September	October	November	December	[a]
pH	7.90	7.95	8.10	7.80	7.90	8.11	8.28	8.60	8.30	7.70	7.70	7.10	7.9 (0.4)
T (°C)	12.0	11.3	16.2	–	21.7	24.9	30.3	–	–	23.8	17.9	10.1	15.9 (9.4)
Eh (mV)	219.8	189.8	209.7	158.4	189.2	196.0	349.3	164.8	148.5	161.2	220.4	221.1	197.7 (40.8)
EC (μS cm^{-1})	2090	1755	1677	2070	2160	1822	1890	1277	1707	1809	1132	1134	1704.1 (352.0)
Hardness (mg $CaCO_3$ L^{-1})	396.5	327.3	303.9	368.6	434.7	398.0	352.2	347.9	427.6	343.9	314.1	225.5	347.1 (51.5)
TAC (mg HCO_3 L^{-1})	132.3	110.0	117.0	154.9	133.7	132.1	152.2	133.9	164.2	114.4	158.9	86.7	132.1 (23.0)
SAR	5.75	5.53	5.30	5.19	6.13	5.26	4.11	4.85	4.79	5.32	3.47	4.18	5.00 (0.68)
Na^+ (mg L^{-1})	263.0	229.8	212.3	228.8	293.9	241.1	177.3	207.8	227.4	226.7	141.3	144.4	214.5 (37.8)
K^+ (mg L^{-1})	6.3	5.0	4.9	5.1	6.5	5.3	4.2	4.6	5.4	5.4	4.1	3.4	5.0 (0.7)
Ca^{2+} (mg L^{-1})	83.6	69.1	65.8	81.5	87	83.8	76.9	71.9	89.6	73.1	67.9	53.2	74.1 (9.5)
Mg^{2+} (mg L^{-1})	45.6	37.5	33.9	40.1	52.8	45.8	38.9	40.9	49.5	39.2	35.1	22.5	39.4 (6.8)
Cl^- (mg L^{-1})	354.1	311.8	281.8	316.9	405.6	349.6	262.4	296.5	342.7	306.9	209.7	185.4	297.5 (51.7)
NO_3^- (mg L^{-1})	44.7	47.7	37.3	27.5	43.4	40.2	27.9	34.9	36.9	41.8	28.9	34.6	36.7 (6.2)
SO_4^{2-} (mg L^{-1})	333.5	271.9	248.2	295.4	364.4	297.8	232.6	260.1	286.9	292.1	166.7	176.4	264.7 (49.3)
HCO_3^- (mg L^{-1})	132.2	110.0	117.1	154.9	133.7	128.4	145.3	94.0	133.9	114.4	159.0	86.8	125.8 (22.7)
CO_3^{2-} (mg L^{-1})	0.0	0.0	0.0	0.0	0.0	0.0	3.4	19.7	14.9	0.0	0.0	0.0	3.1 (6.7)
F^- (mg L^{-1})	0.0	0.0	0.0	0.0	1.00	0.25	0.40	0.50	0.50	0.40	0.40	0.40	0.3 (0.2)

–: not available.

[a] Average (standard deviation).

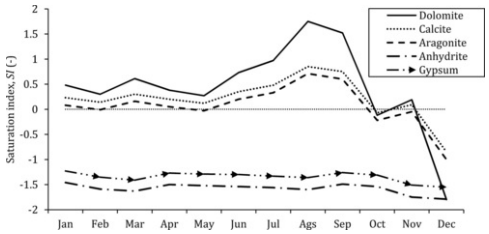

Fig. 4 Temporal evolution of the saturation index *SI* of irrigation water.

5.2 Main scenario: reactive transport and long-term impacts

The transport regime is characterized by two dimensionless numbers. The Péclet number, which compares the relative importance of advective and diffusive effects during transport. Here, computing it as $Pe = (v/D_m)\Delta z$ (e.g., El-Kadi and Ge, 1993), where v is the mean water velocity (L T^{-1}) ($v = q/\theta$), and Δz the spatial discretization (L), 1 cm in this case. The Damkohler number, which compares the mean travel time to the time required to reach the equilibrium, $Da = \Delta z(\theta/q)/(C_{eq,i}/R_i)$, (e.g., Maher and Chamberlain, 2014), where $C_{eq,i}$ is the thermodynamic limit (i.e., the maximum concentration) (M L^{-3}), and R_i is the reaction rate of element i (M L^{-3} T^{-1}). The average Pe is smaller than 1, and the Da for the two main mineral species involved (i.e., calcite and gypsum) is similar to 1. Based on these two criteria, we assume that the geochemical equilibrium is reached between the old resident water, new input water and soil minerals.

Fig. 5a and b, spatio-temporal plots, show predicted mass change content (mol) in the soil profile with time for calcite and gypsum, respectively, compared to the initial values. For better illustration/readability and understanding of the most relevant processes, the soil profile of Fig. 2 is zoomed to 60 cm depth, and not 140 cm depth completed with the numerical simulations. Dolomite, aragonite and anhydrite have not been considered in the evaluation of the soil physical and hydraulic properties changes, since their dynamic of precipitation/dissolution is negligible.

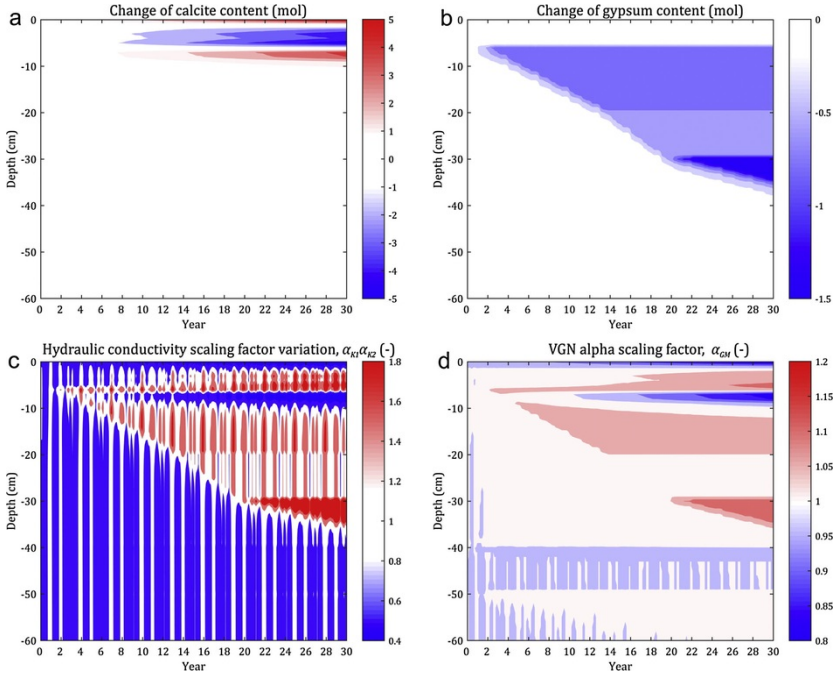

Fig. 5 Space-time plots of expected changes in (a) calcite content (mols), (b) gypsum content (mols), (c) the K_s scaling factor, $\alpha_{k1}\alpha_{k2}$, and (d) the alpha of van Genuchten model scaling factor, α_{GM}, for the reference scenario.

As expected, calcite dissolution/precipitation dynamic is strongly influenced by pCO_2. On the soil surface, at a depth between 0 and 2 cm, precipitation of calcite is expected, leading to a carbonate crust formation. Similar results have been reported by Gran et al. (2011) and Nachshon et al. (2011a,b). Simulation indicates that calcite dissolution will occurs in the root zone, where a maximum pCO_2 of $10^{-1.5}$ atm is adopted considering existing biological activity (Fig. 2). Irrigation water, saturated in calcite under atmospheric conditions

(Table 5 and Fig. 4) and subsaturated in the root zone (between 2- and 6 cm), will dissolve calcite from soil. The mixture of these two different waters, which are both saturated for calcite, but with a different pCO_2, will lead to a water composition that is subsaturated for this mineral (Appelo and Postma, 2005). Below the root zone, between 6 and 10 cm depth, the lower pCO_2 will induce calcite precipitation (Fig. 5a).

Soil gypsum content presents a more regular geochemical behaviour than calcite. The input water, subsaturated in this mineral facies, will imply the continuous dissolution of the available gypsum in the soil profile (Fig. 5b). Gypsum will be completely dissolved by the input water from top to bottom of the soil profile. The horizontal bands are the result of different initial gypsum content in each soil layer defined.

Simulation shows that two main processes control the saturated hydraulic conductivity patterns (Fig. 5c): first, soil water salinity cyclical process and, specially, temperature changes as observed from the vertical bands (seasonal-annual variation of temperature) (Eq. (11)); second, calcite and gypsum dissolution/precipitation (Eq. (14)). The spatio-temporal evolution of the porosity, temperature, water salinity, density and dynamic viscosity, all of them affecting the hydraulic conductivity, are included in the Supplementary Material. Fig. 5d shows the spatio-temporal evolution of the alpha parameter (inversely correlated with air entry into soil matrix) from the van Genuchten model. It is intimately related to changes in porosity (see Supplementary Material), in this case θ_s, according to Eq. (10). The updating of K_s, θ_s and α implies new pressure-saturation curves every time step and depth.

The expected calcite crust formation on the soil surface will mean an upper hydraulic conductivity barrier, with a subsequent reduction of infiltration and direct evaporation. Between 2 and 6 cm depth, porosity changes are consequence exclusively of calcite dissolution since the X-ray mineralogy determinations indicate no gypsum in the top layer (Table 4). Therefore, hydraulic conductivity-scaling factor shows an increase at this depth interval (Fig. 5c). Below the root zone (6–20 cm), gypsum dissolution and calcite precipitation will take place. The effect of gypsum dissolution on porosity (molar volume double than calcite, Table 3) is greater than calcite precipitation. As a result, porosity will increase and also the saturated hydraulic conductivity, so no root growth blockage is expected despite the calcite precipitation below roots. After 30 years of simulation and at higher depths than 20 cm, the expected calcite changes are lower. pCO_2 changes are very important in the upper part of the soil profile, due to atmospheric and root zone influence. Below the root zone, CO_2 ~~concertation~~concentration tends to stabilize, but also soil water content and saturation indexes of the considered minerals. In other words, in the upper part of the soil profile there is a non-steady state (i.e., non-equilibrium), while below the action of the evaporation and roots, the soil reaches a *quasi*-steady state (i.e., *quasi* equilibrium). At long-term and below 20 cm, only gypsum dissolution will be important. Less significant changes are detected at around 40 cm depth, although slow gypsum dissolution is expected to continue for longer times and greater depths.

5.3 Scenarios of environmental conditions

5.3.1 Rain-fed irrigation

Fig. 6 summarises simulation results after considering that irrigation is not applied. As the water input by rainfall is much lower than in the irrigation scenario, all the geochemical processes (dissolution/precipitation) (Fig. 6a and b), and impacts on soil physical (porosity) and hydraulic (conductivity) properties, became less significant. The only observed changes correspond to annual and seasonal temperature impact on the K_s (Fig. 6c), while it is null for α (Fig. 6d). Calcite crust on the soil surface did not build up, highlighting the role of the desalinated water application as a leading factor of soil physical and hydraulic properties changes. Therefore, no affection to infiltration, direct evaporation or root growth are expected, while vegetation death is highly probable due to the semi-arid conditions.

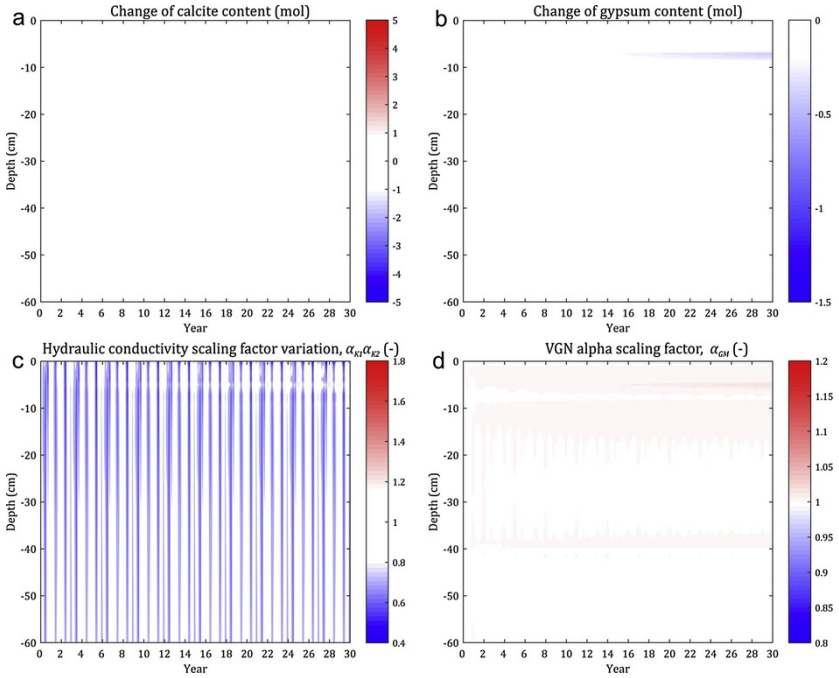

Fig. 6 Space-time plots of expected changes in (a) calcite content (mols), (b) gypsum content (mols), (c) the K_s scaling factor, $\alpha_{k1}\alpha_{k2,}$ and (d) the alpha of van Genuchten model scaling factor, α_{GM}, for the rain-fed scenario.

5.3.2 Absence of gypsum in the soil profile

According to the reference scenario results, gypsum dissolution plays an important role in θ_s and K_s changes, even when considering low initial concentration in the soil profile (gypsum is not present in layer 1, and it is below 7% in layer 2 and under 3% in layer 3).

In a gypsum-free soil profile, calcite will precipitate in the soil surface, as a crust, while it will dissolve within the first few centimetres below the crust; aragonite will also precipitate at this depth (Fig. 7a). The lack of gypsum in the soil profile impairs its dissolution although the infiltrating water is subsaturated in it (Fig. 7b). Compared with the reference scenario: θ_s will be reduced due to calcite precipitation and will not be counterbalanced with gypsum dissolution; and K_s will mainly decrease along the soil profile except in the root zone (Fig. 7c).

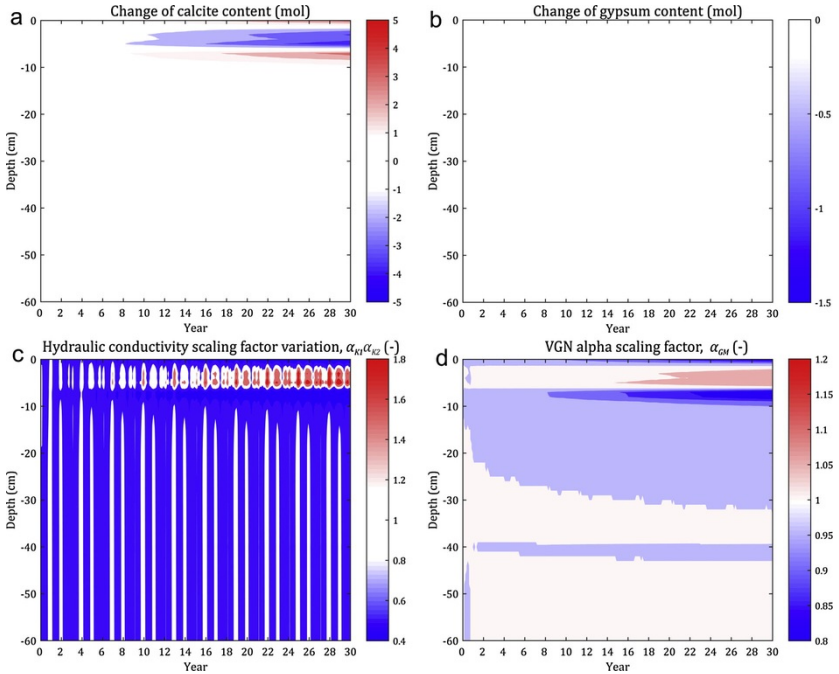

Fig. 7 Space-time plots of expected changes in (a) calcite content (mols), (b) gypsum content (mols), (c) the K_s scaling factor, $\alpha_{k1}\alpha_{k2}$, and (d) the alpha of van Genuchten model scaling factor, α_{GM}, for the gypsum-free soil profile scenario.

The development of a less permeable layer below the root zone (between 6 and 20 cm depth, approximately), with a scaling factor of 0.5 for K_s and 0.8 for the α parameter of van Genuchten model (Fig. 7c and d), will imply the root growth blockage at long-term.

5.3.3 Lower pCO_2 in the root zone

The obtained results are similar to the reference scenario, although processes such as precipitation/dissolution of calcite are of less magnitude (Fig. 8a). The maximum calcite precipitation in the soil surface and below the roots is expected to be reduced from 5 to 3 mol, while calcite dissolution in the root zone from 5 to 2 mol with respect to the reference scenario. Gypsum dynamics is virtually independent of pCO_2 and almost will follow the reference scenario pattern, i.e., all the gypsum available in the soil profile will be gradually dissolved (Fig. 8b). The changes in the K_s and α (Fig. 8c and b) are also similar to the reference scenario. Therefore, no necessarily a reduction of pCO_2 or aeration of the system will imply significant changes in the soil physical and hydraulic properties with respect to the reference scenario.

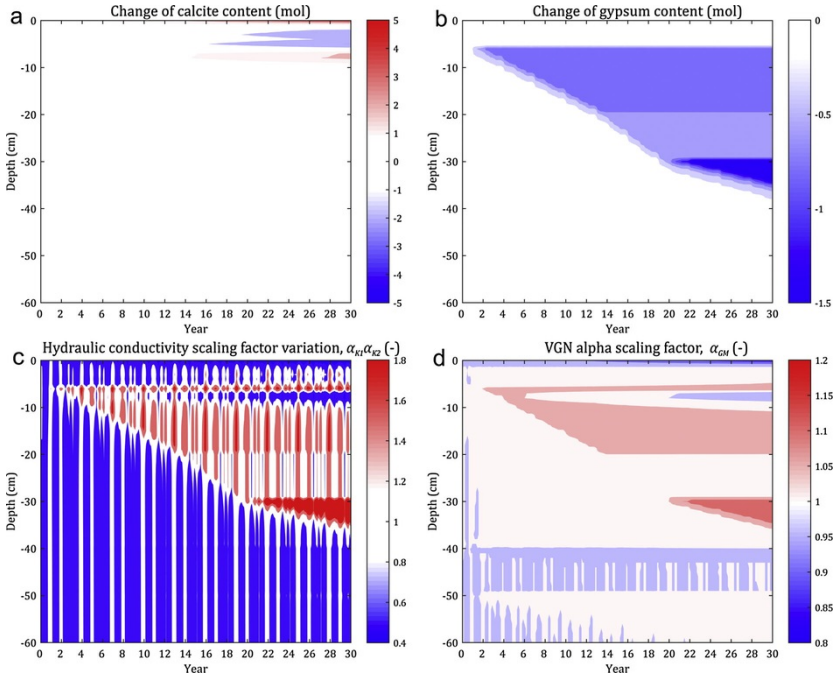

Fig. 8 Space-time plots of expected changes in (a) calcite content (mols), (b) gypsum content (mols), (c) the K_s scaling factor, $\alpha_{k1}\alpha_{k2,}$ and (d) the alpha of van Genuchten model scaling factor, α_{GM}, for the lower partial pressure of CO_2 (pCO_2) in the root zone scenario.

6 Conclusions

Assessment of impacts on soil properties by non-conventional water irrigation is an increasing concern problem. Understanding and integrating all the involved processes, and quantifying the expected impacts can be achieved through numerical process-based modelling. However, the use as starting point of field data, both from soil and boundary conditions, can reduce considerably the associated uncertainty.

This work presents a numerical model that combines water flow, heat and non-isothermal multicomponent reactive transport, along with a self-proposed computation of the spatio-temporal variability in the soil physical and hydraulic properties. The application of this numerical model to evaluate the long-term (i.e., 30 years) impacts on soil from the irrigation with non-conventional water (i.e., desalinated water) in a semi-arid region reveals its potential as a predictive tool. For the particular soil and boundary conditions studied, two aspects stand out: (*i*) the key role played by the partial pressure of CO_2 (atmospherically and biologically controlled), which triggers the precipitation of calcite on the surface and just below the root zone, and the dissolution in between, and (*ii*) the gypsum dissolution in the soil profile, counterbalancing the calcite precipitation. As main expected long-term impacts, for gypsum-bearing soils, as in our case, porosity and saturated hydraulic conductivity will increase along the profile mainly by gypsum dissolution (molar volume of gypsum is double than calcite), except on the surface and below roots due to calcite precipitation. However, this localized calcite precipitation will reduce the direct soil evaporation and could imply the root growth blockage.

Other probable scenarios, beside the reference case, considering different initial and boundary conditions have also been proposed based on their interest for the region. The different scenarios results have demonstrated the importance of individual components: (*i*) the rain-fed scenario (i.e., no irrigation) shows that the use of low quality irrigation water (desalinated water, subsaturated in gypsum) will trigger most of the reactions; (*ii*) in the gypsum-free soil profile scenario, a carbonate crust formation on the surface and below the root zone is expected to occur, with a potential reduction by a factor 2 and 0.2 of the saturated hydraulic conductivity and the alpha parameter of van Genuchten model, respectively, since the porosity reduction by calcite precipitation is not counterbalanced by gypsum dissolution; and (*iii*) a lower partial pressure of CO_2 scenario shows an expected reduction in the calcite precipitation on the surface and below the roots, while changes in the soil physical and hydraulic properties are expected to be similar to the reference case, since gypsum dissolution is the main control on them.

Although results and conclusions depend on specific local conditions, including soil mineralogy, irrigation water quality and climate, among others, obtained results can contribute to improve understanding of processes in similar regions. Note that such a modelling approach forms a basis for studying climate change effects either through the methodology of climatic analogues (Leterme et al., 2012) or the generation of climate change scenarios (Candela et al., 2009); the evaluation in detail of the relative importance of climate change in the studied processes needs to be addressed in further investigations.

7 Uncited reference

~~Xue et al. (2003).~~

Acknowledgements

This study forms part of the CGL2010-22168-C03/BTE and CGL2013-48802-C3-3-R projects, financed by the Spanish Ministry of Economy and Competitiveness, and of the GRE15-19 project financed by the University of Alicante (Spain). Gratitude is also expressed to Dr. Iñaki Vadillo from the University of Malaga (Spain); the IMDEA-AGUA and Dr. Ignasi Queralt from the IDAEA-CSIC (Spain).

Appendix A. Supplementary material

Supplementary data associated with this article can be found, in the online version, at http://dx.doi.org/10.1016/j.jhydrol.2017.03.061.

References

Abderrahim H., Candela L., Queralt I., Tamoh K. and Maslouhi A., X-ray fluorescence analysis for total bromine tracking in the vadose zone: results for Mnsara, Morocco, *Vadose Zone J.* **10**, 2011, 1331–1335.

Allen R.G., Pereira L.S., Raes D. and Martin S., Crop Evapotranspiration - Guidelines for Computing Crop Water Requirements - FAO Irrigation and Drainage Paper 56, 1998, Food and Agriculture Organization of the United Nations; Rome.

Appelo C.J. and Postma D., Geochemistry Groundwater and Pollution, second ed., 2005, Taylor & Francis Group.

Assouline S. and Narkis K., Effects of long-term irrigation with treated wastewater on the hydraulic properties of a clayey soil, *Water Resour. Res.* **47** (8), 2011, http://dx.doi.org/10.1029/2011WR010498.

Assouline S. and Narkis K., Effect of long-term irrigation with treated wastewater on the root zone environment, *Vadose Zone J.* **12** (2), 2013, http://dx.doi.org/10.2136/vzj2012.0216.

Ball, J.W., Nordstrom D.K., 1991. WATEQ4F-User's manual with revised thermodynamic data base and test cases for calculating speciation of major trace and redox elements in natural waters. U. S. Geological Service, Menlo Park, CA.

Bouwer H., Artificial recharge of groundwater: Hydrogeology and engineering, *Hydrogeol. J.* **10**, 2002, 121–142.

Brindley G.W. and Brown G., Crystal Structures of Clay Minerals and Their X-Ray Identification, 1980, Mineralogical Society of Great Britain and Ireland; Middlesex (UK), 495.

Candela L., von Igel W., Javier Elorza F. and Aronica G., Impact assessment of combined climate and management scenarios on groundwater resources and associated wetland (Majorca, Spain), *J. Hydrol.* **376**, 2009, 510–527.

Costa J.L., Effect of irrigation water quality under supplementary irrigation on soil chemical and physical properties in the 'Southern Humid Pampas' of Argentina, *J. Crop Prod.* **2**, 1999, 85–99.

Chung S.-O. and Horton R., Soil heat and water flow with a partial surface mulch, *Water Resour. Res.* **23**, 1987, 2175–2186.

Dane J.H. and Hopmans J.W., Pressure plate extractor, In: Dane J. and Topp C., (Eds.), *Methods of Soil Analysis, Part 4 Physical Methods,* 2002, Soil Science Society of America; Madison, WI (USA), 688–690.

de Marsily, G., 1986. Quantitative hydrogeology. Academic Press, London (UK). 464 p. ISBN: 9780122089169.

de Vries D.A., The thermal properties of soils, In: van Wijk R.W., (Ed), *Physics of Plant Environment,* 1963, North-Holland Books Co.; North Holland (Amsterdam), 210–235.

El-Kadi A.I. and Ge L., The Courant and Peclet number criteria for the numerical solution of the Richards equation, *Water Resour. Res.* **29** (10), 1993, 3485–3494.

Feddes R.A., Kowalik P.J. and Zaradny H., Simulation of Field Water Use and Crop Yield, 1978, Wiley; New York, NY (USA), 188.

Flint, A.L. Flint, L.E., 2002. Porosity. In: Dane, J., Topp, C. (Eds.), Methods of soil analysis. Part 4. Physical methods. Soil Science Society of America, Madison, WI (USA), pp. 241–253.

Francisca F.M. and Glatstein D.A., Long term hydraulic conductivity of compacted soils permeated with landfill leachate, *Appl. Clay Sci.* **49** (3), 2010, 187–193.

Gee, G.W., Or, D., 2002. Particle-Size Analysis. In: Dane, J., Topp, C. (Eds.), Methods of soil analysis. Part 4. Physical methods. Soil Science Society of America, Madison, WI (USA), pp. 255–293.

Gran M., Carrera J., Olivella S. and Saaltink M.W., Modeling evaporation processes in a saline soil from saturation to oven dry conditions, *Hydrol. Earth Syst. Sci.* **15**, 2011, 2077–2089.

Grossman, R.B., Reinsch, T.G., 2002. Bulk density and linear extensibility. In: Dane, J., Topp, C. (Eds.), Methods of soil analysis. Part 4. Physical methods. Soil Science Society of America, Madison, WI (USA), pp. 201–228.

Jacques D., Šimůnek J., Mallants D. and van Genuchten M.T., Operator-splitting errors in coupled reactive transport codes for transient variably saturated flow and contaminant transport in layered soil profiles, *J. Contam. Hydrol.* **88**, 2006, 197–218.

Jacques D., Šimůnek J., Mallants D. and van Genuchten M.T., Modeling coupled hydrologic and chemical processes: long-term uranium transport following phosphorus fertilization, *Vadose Zone J.* **7**, 2008, 698–711.

Jacques, D., Šimůnek, J., Mallants, D., van Genuchten, M.T., Li, Y., 2011. A coupled reactive transport model for contaminant leaching from cementitious waste matrices accounting for solid phase alterations. In: Thirteenth Internationa Waste Management and Landfill Symposium, S. Margherita di Pula, Cagliari (Italy). CISA Publisher, Sardinia 2011, 3–7 October 2011.

Jones A., X-Ray Fluorescence Analysis, In: Smith K.A., (Ed), *Soil Analysis,* 1991, Modern Instrumental Techniques; Marcel Dekker, New York, NY (USA), 287–324.

Kanzari S., Hachicha M., Bouhlila R. and Battle-Sales J., Characterization and modeling of water movement and salts transfer in a semi-arid region of Tunisia (Bou Hajla, Kairouan) - salinization risk of soils and aquifers, *Comput. Electron. Agr.* **86**, 2012, 34–42.

Lado M. and Ben-Hur M., Effects of irrigation with different effluents on saturated hydraulic conductivity of arid and semiarid soils, *Soil Sci. Soc. Am. J.* **74**, 2010, 23–32.

Lee R.W., Effects of carbon dioxide variations in the unsaturated zone on water chemistry in a gracial/outwash aquifer, *Appl. Geochem.* **12**, 1997, 347–366.

Lahav O., Kochva M. and Tarchitzky J., Potential drawbacks associated with agricultural irrigation with treated wastewaters from desalinated water origin and possible remedies, *Water Sci. Technol.* **61**, 2010, 2451–2460.

Leterme B., Mallants D. and Jacques D., Sensitivity of groundwater recharge using climatic analogues and HYDRUS-1D, *Hydrol. Earth Syst. Sci.* **16**, 2012, 2485–2497.

Loisy C., Cohen G., Laveuf C., Le Roux O., Delaplace P., Magnier C., Rouchon V., Cerepi A. and Garcia B., The CO_2-Vadose Project: dynamics of the natural CO_2 in a carbonate vadose zone, *Int. J. Greenh. Gas Control* **14**, 2013, 97–112.

Maher K. and Chamberlain C.P., Hydrologic regulation of chemical weathering and the geologic, *Science* **343** (6178), 2014, 1502–1504.

Martínez Beltrán, J., Koo-Oshima, S., 2004. Water desalination for agricultural applications. In: Proceedings of the FAO Expert Consultation on Water Desalination for Agricultural Applications 26–27 April 2004, Rome. Food and Agriculture Organization of the United Nations, FAO, Rome.

MedWSD Working Group, 2007. Mediterranean Water Scarcity and Drought Report. European Commission. Euro-Mediterranean Information System on know-how in the Water sector.

Millington R.J. and Quirk J.P., Permeability of porous solids, *Trans. Faraday Soc.* **57**, 1961, 1200–1207.

Minhas P.S., Naresh R.K., Chauhan C.P.S. and Gupta R.K., Field determined hydraulic properties of a sandy loam soil irrigated with various salinity and SAR waters, *Agric. Water Manage.* **25**, 1994, 97–108.

Mualem Y., A new model for predicting the hydraulic conductivity of unsaturated porous media, *Water Resour. Res.* **12**, 1976, 513–522.

Nachshon U., Shahraeeni E., Or D., Dragila M. and Weisbrod N., Infrared thermography of evaporative fluxes and dynamics of salt deposition on heterogeneous porous surfaces, *Water Resour. Res.* **47** (12), 2011a, http://dx.doi.org/10.1029/2011WR010776.

Nachshon U., Weisbrod N., Dragila M.I. and Grader A., Combined evaporation and salt precipitation in homogeneous and heterogeneous porous media, *Water Resour. Res.* **47** (3), 2011b, http://dx.doi.org/10.1029/2010WR009677.

Nelson, D.W., Sommers, L.E., 1996. Total Carbon, Organic Carbon, and Organic Matter. In: Sparks, D.L. (Ed.), Methods of Soil Analysis. Part 3. Chemical and Microbiological Properties. Soil Science Society of America, Madison, WI, USA, pp. 961–1010.

Parkhurst, D.L., Appelo, C.A.J., 2013. Description of Input and Examples for PHREEQC Version 3-A Computer Program for Speciation, Batch-Reaction, One-Dimensional Transport, and Inverse Geochemical Calculations. U.S. Geological Service, Denver, Colorado.

Phogat V., Yadav A.K., Malik R.S., Kumar S. and Cox J., Simulation of salt and water movement and estimation of water productivity of rice crop irrigated with saline water, *Paddy Water Environ.* **8**, 2010, 333–346.

Prats D. and Chillón Arias M.F., A reverse osmosis potable water plant at Alicante University: first years of operation, *Desalination* **137**, 2001, 91–102.

Prats D., Chillón M.F., Rubio M. and Reverte J.A., Alicante University, closed water cycle, reverse osmosis and water treatment plants, *Desalination* **109**, 1997, 315–321.

Qadir M., Sharma B.R., Bruggeman A., Choukr-Allah R. and Karajeh F., Non-conventional water resources and opportunities for water augmentation to achieve food security in water scarce countries, *Agric. Water Manage.* **87**, 2007, 2–22.

Ramos T.B., Šimůnek J., Gonçalves M.C., Martins J.C., Prazeres A. and Castanheira N.L., Field evaluation of a multicomponent solute transport model in soils irrigated with saline waters, *J. Hydrol.* **407**, 2011, 129–144.

Reading L.P., Baumgartl T., Bristow K.L. and Lockington D.A., Applying HYDRUS to flow in a Sodic clay soil with solution composition-dependent hydraulic conductivity, *Vadose Zone J.* **11** (2), 2012a, http://dx.doi.org/10.2136/vzj2011.0137.

Reading L.P., Baumgartl T., Bristow K.L. and Lockington D.A., Hydraulic conductivity increases in a sodic clay soil in response to gypsum applications: impacts of bulk density and cation exchange, *Soil Sci.* **177** (3), 2012b, 165–171.

Reynolds, W.D., Elrick, D.E., 2002. Constant head soil core (tank) method. In: Dane, J., Topp, C. (Eds.), Methods of soil analysis. Part 4. Physical methods. Madison, WI, USA, pp. 804–808.

Richards L.A., Capillary conduction of liquids through porous mediums, *J. Appl. Phys.* **1**, 1931, 318–333.

Sani A., Scholz M., Babatunde A. and Wang Y., Impact of water quality parameters on the clogging of vertical-flow constructed wetlands treating urban wastewater, *Water Air Soil Pollut.* **224** (3), 2013, http://dx.doi.org/10.1007/s11270-013-1488-2.

Sharqawy M.H., Lienhard V.J.H. and Zubair S.M., Thermophysical properties of seawater: a review of existing correlations and data, *Desalin. Water Treat.* **16** (1–3), 2010, 354–380, http://dx.doi.org/10.5004/dwt.2010.1.

Šimůnek J., Jacques D., van Genuchten M.T. and Mallants D., Multicomponent geochemical transport modeling using HYDRUS-1D and HP1, *J. Am. Water Resour. Assoc.* **42**, 2006, 1537–1547.

Šimůnek, J., Šejna, M., Saito, H., Sakai, M., van Genuchten, M.T., 2009. The HYDRUS-1D Software Package for Simulating the Movement of Water, Heat, and Multiple Solutes in Variability Saturated Media, Version 4.08. Department of Environmental Sciences. University of California, Riverside, CA, USA.

Steefel C.I., Appelo C.A.J., Arora B., Jacques D., Kalbacher T., Kolditz O., Lagneau V., Lichtner P.C., Mayer K.U., Meeussen J.C.L., Molins S., Moulton D., Shao H., Šimůnek J., Spycher N., Yabusaki S.B. and Yeh G.T., Reactive transport codes for subsurface environmental simulation, *Comput. Geosci.* **19** (3), 2015, 445–478, http://dx.doi.org/10.1007/s10596-014-9443-x.

Sumner M.E. and Miller W.P., Cation exchange capacity and exchange coefficients, In: Sparks D.L., (Ed), *Methods of Soil Analysis, Part 3. Chemical Methods,* 1996, Soil Science Society of America, 1201–1230.

Tal A., Seeking sustainability: Israel's evolving water management strategy, *Science* **313**, 2006, 1081–1084.

Valdes-Abellan J., Candela L., Jiménez-Martínez J. and Saval-Pérez J.M., Brackish groundwater desalination by reverse osmosis in southeastern Spain. Presence of emerging contaminants and potential impacts on soil-aquifer media, *Desal. Water Treat.* **51**, 2013, 2431–2444.

Valdes-Abellan J., Jiménez-Martínez J. and Candela L., Dispersivity determination through a modeling approach from a tracer test based on total br concentration in soil samples, *Soil Sci.* **179**, 2014, 403–408.

Valdes-Abellan J., Jiménez-Martínez J., Candela L. and Tamoh K., Comparison among monitoring strategies to assess water flow dynamic and soil hydraulic properties in agricultural soils, *Span. J. Agric. Res.* **13** (1), 2015, http://dx.doi.org/10.5424/sjar/2015131-6323.

van Genuchten M.T., Closed-form equation for predicting the hydraulic conductivity of unsaturated soils, *Soil Sci. Soc. Am. J.* **44**, 1980, 892–898.

Wesseling J.G. and Brandyk T., Introduction of the Occurrence of High Groundwater Levels and Surface Water Storage in Computer Program SWATRE, 1985, Instituut voor Cultuurtechniek en Waterhuishouding; ICW, Wageningen.

Wissmeier L. and Barry D.A., Effect of mineral reactions on the hydraulic properties of unsaturated soils: model development and application, *Adv. Water Resour.* **32** (8), 2009, 1241–1254.

Wissmeier L. and Barry D.A., Implementation of variably saturated flow into PHREEQC for the simulation of biogeochemical reactions in the vadose zone, *Environ. Model. Softw.* **25** (4), 2010, 526–538.

Xu J., Wu L., Chang A.C. and Zhang Y., Impact of long-term reclaimed wastewater irrigation on agricultural soils: a preliminary assessment, *J. Hazard. Mater.* **183**, 2010, 780–786.

Xue Q., Zhu Z., Musick J.T., Stewart B.A. and Dusek D.A., Root growth and water uptake in winter wheat under deficit irrigation, *Plant Soil* **257**, 2003, 151–161.

Appendix A. Supplementary material

Multimedia Component 1

Supplementary data 1

Highlights

- Non-isothermal multicomponent reactive transport with spatio-temporal variability of soil physical and hydraulic properties.
- Long-term impacts of non-conventional water irrigation on soil.
- Root zone control on partial pressure of CO_2 and precipitation/dissolution of calcite.
- User-friendly numerical tool for water management, irrigation strategies and water policy makers.

Queries and Answers

Query: Please crossrefer footnotes " and **" in Table 1.
Answer: Done

Query: Your article is registered as a regular item and is being processed for inclusion in a regular issue of the journal. If this is NOT correct and your article belongs to a Special Issue/Collection please contact g.suresh@elsevier.com immediately prior to returning your corrections.
Answer: The article does not belong to a Special Issue

Query: The author names have been tagged as given names and surnames (surnames are highlighted in teal color). Please confirm if they have been identified correctly.
Answer: The names are correct.

Query: References 'Xie et al. (2015)' is cited in the text but not provided in the reference list. Please provide it in the reference list or delete this citation from the text.
Answer: Xie M., Ulrich, K., Mayer U., Claret F., Alt-Epping P., Jacques D., Steefel C., Chiaberge C., and Šimůnek J., Implementation and evaluation of permeability-porosity and tortuosity-porosity relationships linked to mineral dissolution-precipitation. *Comput. Geosci.*, **19**(3), 655–671, 2015, http://dx.doi.org/10.1007/s10596-014-9458-3

Query: The citation 'Sumner et al. (1996)' has been changed to 'Sumner and Miller (1996)' to match the author name in the reference list. Please check here and in subsequent occurrences, and correct if necessary.
Answer: We agree the change

Query: The citation 'Loisy et al. (2003)' has been changed to 'Loisy et al. (2013)' to match the year in the reference list. Please check here and in subsequent occurrences, and correct if necessary.
Answer: We agree the change

Query: This section comprises references that occur in the reference list but not in the body of the text. Please position each reference in the text or, alternatively, delete it. Any reference not dealt with will be retained in this section.
Answer: The reference has to be deleted from the reference list.

Query: The country names of the Grant Sponsors are provided below. Please check and correct if necessary. 'University of Alicante' - 'Spain'.
Answer: Corrected in the text

Query: One or more sponsor names may have been edited to a standard format that enables better searching and identification of your article. Please check and correct if necessary.
Answer: We consider that the sponsors name are correct